Activation Mechanism of CDK2: Role of Cyclin Binding versus Phosphorylation†

Lisa M. Stevenson,‡ Michael S. Deal,§ Jonathan C. Hagopian,§ and John Lew*,‡

Department of Molecular, Cellular and Developmental Biology and Program in Biomolecular Sciences and Engineering, University of California, Santa Barbara, California 93106

Received March 14, 2002; Revised Manuscript Received May 7, 2002

ABSTRACT: Activation of the cyclin-dependent kinases is a two-step process involving cyclin binding followed by phosphorylation at a conserved threonine residue within the kinase activation loop. In this study, we describe the separate roles of cyclin A binding versus phosphorylation in the overall activation mechanism of CDK2. Interaction of CDK2 with cyclin A results in a partially active complex that is moderately defective in the binding of the protein substrate, but not ATP, and severely defective in both phosphoryl group transfer and turnover. Alternatively, phosphorylation of the CDK2 monomer also results in a partially activated species, but one that is severely (≥480-fold) defective in substrate binding exclusively. Catalytic turnover in the phosphorylated CDK2 monomer is largely unimpaired (∼8-fold lower). Our data support a model for the activation of CDK2 in vivo, in which interaction of unphosphorylated CDK2 with cyclin A serves to configure the active site for ground-state binding of both ATP and the protein substrate, and further aligns ATP in the transition state for phosphoryl transfer. Optimizing the alignment of protein substrates in the phosphoryl transfer reaction is the principal role of phosphorylation at Thr^{160}.

Cell proliferation is controlled by a family of enzymes known as the cyclin-dependent protein kinases whose catalytic activities are regulated in a cyclic fashion during progression through the eukaryotic cell division cycle (*1*). Classically, the mitotic CDKs[1] are activated by a two-step process involving cyclin binding followed by phosphorylation at a conserved threonine residue located within the kinase activation loop. While cyclin B-bound CDK1 serves to control progression across the G2−M phase boundary of the cell cycle, CDK2 bound to cyclin E or A controls progression across the G1−S phase boundary or through the S phase, respectively (*1*, *2*). Although cyclin B-bound CDK1 was the first to be discovered and biochemically characterized, high-resolution structural information has been accrued primarily on CDK2. In particular, the crystal structures of all partially activated forms of CDK2 are available (*3*−*7*), providing the most detailed view of the structural basis for catalytic activation in a protein kinase (see ref *8* for review).

The catalytic cores of all protein kinases display a bilobal tertiary fold whose interface defines the active site cleft. The adenine ring of ATP binds deep within the cleft, while the γ-phosphate points to the mouth of the cleft where the activation loop is located, and where protein substrates bind (*9*). Comparative analysis of several CDK2 structures has established putative roles for cyclin binding (*3*, *5*) and Thr^{160} phosphorylation (*4*, *7*) in catalytic activation. Interaction with cyclin A optimally aligns the PSTAIRE active site helix and causes dramatic movement of the CDK2 activation loop (*3*, *5*). Full activation requires Thr^{160} phosphorylation, which causes further changes to the activation loop structure (*4*) promoting optimized substrate binding (*7*).

Currently, the crystal structures of more than 20 different protein kinases have been determined.[2] By comparison, the paucity of kinetic data describing their catalytic reaction pathways and mechanisms of regulation has hindered a rigorous correlation of structure with biological function. To address this, we previously determined the catalytic reaction pathway of CDK2 bound to cyclin A and the kinetic basis for activation by phosphorylation (*10*). Here, we describe the individual roles of cyclin binding separate from that of phosphorylation in the overall activation pathway. The data provide a relatively complete picture of the activation mechanism of CDK2.

MATERIALS AND METHODS

Protein Expression and Purification

Human CDK2 (GST−CDK2) in pGEX2T (Pharmacia) and bovine cyclin A3 (corresponding to residues 171−432 in human cyclin A) in pET21d (cyclin A-His_6) were expressed in *Escherichia coli* strain BL21(DE3) as previously described (*10*). The [unP]CDK2−cyclin A complex was generated by colysis of cells separately expressing GST−CDK2 and cyclin A-His_6 and purification by glutathione−agarose chromatography followed by thrombin cleavage and

† This work was supported by National Institutes of Health Grant GM59445. L.M.S. was supported by the UC Santa Barbara Program in Biomolecular Sciences and Engineering Merit Fellowship.

* To whom correspondence should be addressed. Telephone: (805) 893-5336. Fax: (805) 893-4724. E-mail: lew@lifesci.ucsb.edu.

‡ Program in Biomolecular Sciences and Engineering.

§ Department of Molecular, Cellular and Developmental Biology.

[1] Abbreviations: CDK, cyclin-dependent kinase; [T^{160}-P]CDK2−cyclin A, CDK2−cyclin A complex phosphorylated at threonine 160; [unP]CDK2−cyclin A, unphosphorylated CDK2−cyclin A complex; [T^{160}-P]CDK2, monomeric CDK2 phosphorylated at threonine 160; [unP]CDK2, monomeric unphosphorylated CDK2; CAK, CDK-activating kinase; GST, glutathione *S*-transferase.

[2] Protein Kinase Resource Data Base (www.pkr.sdsu.edu).

10.1021/bi025812h CCC: $22.00
Published on Web 06/06/2002

FPLC on Uno Q (Bio-Rad) (*10*). [unP]CDK2 monomer was generated by the same procedure except cell lysis was carried out in the absence of cyclin A-His_6. Column fractions containing [unP]CDK2 monomer were identified by assaying the kinase activity (see below) of each fraction in the presence of separately purified cyclin A-His_6. The [T^{160}-P]-CDK2−cyclin A complex was generated by phosphorylation of purified CDK2 monomer using recombinant yeast GST−CAK1, followed by reconstitution with Ni^{2+}−agarose-purified cyclin A-His_6 (*10*) based on the original protocol by Brown et al. (*6*). Alternatively, strain BL21(DE3) was cotransformed with plasmids separately encoding GST−CDK2 and GST−CAK1, under ampicillin and kanamycin resistance, respectively. Bacteria were grown in LB medium containing ampicillin (100 μg/mL) and kanamycin (50 μg/mL) to an OD_{600} of 0.6−0.8 at 37 °C, and protein expression was induced with 0.4 mM IPTG for 20 h at 23 °C. Purification of the CDK2 monomer (phosphorylated) and in vitro reconstitution with cyclin A-His_6 were carried out as described by Hagopian et al. (*10*). The coexpression procedure gave a 5−10-fold greater yield of the [T^{160}-P]CDK2−cyclin A complex per liter of bacterial culture than that produced by in vitro phosphorylation. For both the purified [unP]CDK2−cyclin A and [T^{160}-P]CDK2−cyclin A complexes, the CDK2:cyclin A ratio was approximately 1:1 as estimated by SDS−PAGE analysis. [T^{160}-P]CDK2 used in kinetic studies was generated as described by Brown et al. (*6*). Enyzme concentrations were determined using SDS−PAGE analysis followed by Coomassie staining and densitometry using BSA as a standard. Alternatively, a colorimetric protein determination assay (BCA, Pierce) was used. Both methods gave corroborating results.

Kinetic Experiments

Kinase Assays. Steady-state catalysis was assessed by incorporation of ^{32}P from [γ-^{32}P]ATP (200−300 cpm/pmol) into either peptide 1 (PKTPKKAKKL) or histone H1 (Sigma, H5505) at room temperature (23 °C). All kinetic experiments were carried out in standard "phosphorylation buffer" [20 mM MOPS (pH 7.4), 50 mM KCl, 0.1 mM EDTA, 1 mM DTT, and 10 mM $MgCl_{2(free)}$] in a 20 μL reaction volume. Reactions were terminated by addition of 5 μL of acetic acid (20% final), and [γ-^{32}P]ATP was separated from the reaction products by ascending chromatography on P81 phosphocellulose paper (Whatman), as previously described (*11*). The amount of ^{32}P incorporated into the product was determined by Cerenkov counting. Since the ATPase activity of the [unP]-CDK2−cyclin A complex is 20-fold higher than the corresponding kinase activity (*10*), an ATP regeneration system [1 mM phosphoenolpyruvate (Sigma, P0564) and 7.5 units/mL pyruvate kinase (Sigma, P7768)] was employed. In this system, the [γ-^{32}P]ATP specific radioactivity decreases over the reaction time course according to simple first-order kinetics dictated by the rate constant k, where $k = v_{ADP}/[ATP]$, v_{ADP} being the rate of ADP formation at a given concentration of ATP. v_{ADP} was calculated from the enzyme concentration and the known steady-state parameters for the ATPase reaction of the [unP]CDK2−cyclin A complex using the Michaelis−Menten equation (*10*). The calculated rate constant (k) was used to correct for the decay in [γ-^{32}P]ATP specific radioactivity in all assays of the [unP]CDK2−cyclin A complex.

To determine if the decay in [γ-^{32}P]ATP specific radioactivity could indeed be accurately modeled, the rate of turnover of total ATP in a typical experiment was determined. A reaction cocktail (140 μL) containing 1 μM [unP]-CDK2−cyclin A complex and 100 μM ATP (250 cpm/pmol by Cerenkov counting) in phosphorylation buffer was prepared, and ATPase activity was allowed to proceed in the presence of an ATP regenerating system (see above). At 0, 2, 4, 8, 16, and 32 min, 20 μL of the reaction mix was removed and the reaction quenched with 5 μL of glacial acetic acid; 1 μL of the stopped reaction mixture was subject to thin-layer chromatography on PEI-cellulose plates (F-254, Selecto Scientific, catalog no. 11078) in 1 M Na_2HPO_4 (pH 3.4). Radioactivity corresponding to ATP was quantified by phosphorimager analysis (Bio-Rad Personal FX). The optimized first-order rate constant for the decay in ATP specific radioactivity as a function of time was determined by regression analysis, and was found to correspond exactly to v_{ADP}/ATP, as predicted by mathematical simulation (data not shown).

Solvent Viscosometric Studies. Steady-state kinetic assays were carried out as described above in buffer containing fixed, increasing amounts of sucrose or fructose, corresponding to relative solvent viscosities varying between 1 and ∼4 (0−40% viscosogen). The relative solvent viscosity was determined as previously described (*11*). Under these conditions, the concentration of one substrate was varied under conditions of saturating (or near-saturating) concentrations of the second.

Effect of Cyclin A on [unP]CDK2 ATPase Activity. The GST−[unP]CDK2 complex (300 μL of an ∼5 μM solution) was incubated with 100 μL of glutathione−agarose beads for 1 h at 4 °C with agitation in a microcentrifuge tube. The beads were pelleted by centrifugation and washed extensively with buffer A [20 mM MOPS (pH 7.4) and 20 mM NaCl] and then loaded into a small spin column. Cyclin A-His_6 (400 μL of an ∼100 μM solution, purified as described above), or buffer, was applied by gravity over the column three times and then spun to remove the excess. The beads were washed with 1.5 mL of buffer B (20 mM MOPS and 250 mM NaCl) and 1.5 mL of buffer A before elution in 100 μL of buffer A and 10 mM glutathione. ATP hydrolysis was monitored in a coupled spectrophotometric assay in which the production of ADP was coupled to the stoichiometric oxidation of NADH, catalyzed by pyruvate kinase and lactate dehydrogenase (*11*). The reaction rate was determined from the rate of decrease in absorbance of NADH at 340 nm [ϵ_{340}(NADH) = 6220 M^{-1} cm^{-1}].

Data Analysis

Steady-state parameters were determined by nonlinear least-squares regression analysis of initial velocity data using the Michaelis−Menten equation describing the addition of one substrate (with the second substrate held at saturation) or, alternatively, the sequential addition of two substrates. In the latter case, eq 1 was globally fit to the data using the software program Scientist (Micromath, Salt Lake City, UT)

$$v = VAB/(K_{iA}K_{mB} + K_{mB}A + K_{mA}B + AB) \qquad (1)$$

where v is the initial velocity, V is the maximal velocity, A is the concentration of the fixed substrate, B is the concentra-

Scheme 1

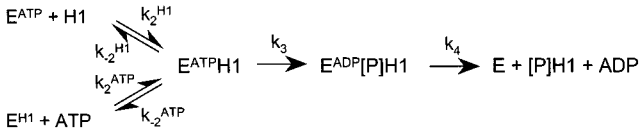

tion of the varied substrate, K_m is the Michaelis constant, and K_{iA} is the dissociation constant for A. k_{cat} was determined by dividing V by the enzyme concentration.

Solvent viscosity data were analyzed according to eq 2, which is derived by combining the Michealis−Menten equation, expressed as a function of the individual reaction steps, and Stokes law (*12*):

$$v = (k_2/\eta)(k_3)(k_4/\eta)(E)(S)/[(k_4/\eta)(k_{-2}/\eta + k_3) + S(k_2/\eta)(k_3 + k_4/\eta)] \quad (2)$$

where E and S are the concentrations of the enzyme and varied substrate, respectively, and η is the relative solvent viscosity. The kinetic constants k_2, k_{-2}, k_3, and k_4, as defined in Scheme 1, relate to the steady-state parameters as follows:

$$k_{cat} = (k_3k_4)/(k_3 + k_4) \quad (3)$$

$$k_{cat}/K_m = (k_2k_3)/(k_{-2} + k_3) \quad (4)$$

Equation 2 was globally fit to initial rate viscosity data, and a set of best-fit curves was obtained by nonlinear regression analysis. The apparent values for k_{cat} and k_{cat}/K_m at each viscosogen concentration were determined, and the fold decreases in k_{cat} and k_{cat}/K_m were plotted as a linear function of the relative solvent viscosity (not shown). The corresponding slope values provide the viscosity effect (denoted by a superscript η) on k_{cat} and k_{cat}/K_m, defined as

$$k_{cat}^{\eta} = k_3/(k_3 + k_4) \quad (5)$$

$$k_{cat}/K_m^{\eta} = k_3/(k_{-2} + k_3) \quad (6)$$

The optimal values for k_2, k_{-2}, k_3, and k_4 were determined from the simultaneous solution to eqs 3−6. Figures 1−5 each represent a typical data set of two to four replicate experiments. All values reported in Tables 1−3 represent the mean obtained from replicate data sets.

In a solvent viscosometric analysis, it is imperative to show that the viscosogen affects only the rate of molecular diffusion, and does not erroneously perturb the enzyme or substrate structure. We have shown that this is true with CDK2 based on the following evidence. (1) The k_{cat} value for the ATPase reaction of the [T^{160}-P]CDK2−cyclin A complex is not affected by high sucrose concentrations (*10*). In the case of the [unP]CDK2−cyclin A complex, sucrose resulted in significant catalytic activation; thus, fructose was employed. Fructose had no effect on k_{cat} for the turnover of histone H1 by the [unP]CDK2−cyclin A complex. Thus, the structure of the CDK2 active site is unperturbed by this viscosogen. (2) Sucrose does not affect the structure of ATP, since $k_{cat}/K_{m(ATP)}$ for [unP]ERK2 is unchanged in sucrose (*13*). (3) The observed viscosity effect on $k_{cat}/K_{m(ATP)}$ in the kinase reaction is not due to competition of the viscosogen with ATP for the active site, because no viscosity effect on this parameter was observed in the ATPase reaction (data not shown).

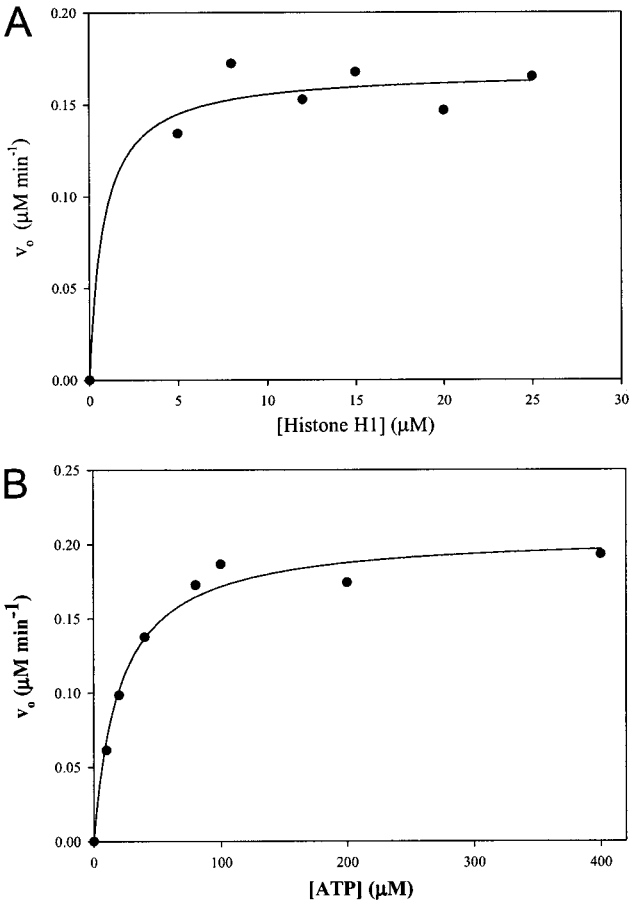

FIGURE 1: Dependence of the initial velocity of the [T^{160}-P]CDK2−cyclin A complex on ATP and histone H1 concentration. Steady-state assays of histone H1 phosphorylation were performed in (A) saturating (1 mM) ATP and varied histone H1 or (B) saturating (20 μM) H1 and varied ATP. In each case, the best-fit curve (see Materials and Methods) is shown. The optimized steady-state kinetic parameters are listed in Table 2. The concentration of the [T^{160}-P]CDK2−cyclin A complex was 2 nM.

RESULTS

Phosphorylation of the CDK2−Cyclin A Complex Does Not Affect ATP Binding Affinity or Reactivity. We previously described the kinetic effects of phosphorylation at Thr^{160} on the CDK2−cyclin A complex with respect to substrate binding and turnover (*10*). Here, we have investigated the effects of phosphorylation on the binding affinity of ATP. While we previously employed a synthetic peptide as the phosphoacceptor substrate (*10*), in these studies we have used histone H1 because of its lower K_m values toward both the [T^{160}-P]CDK2−cyclin A and [unP]CDK2−cyclin A complexes (Table 2). Using either substrate, similar kinetic parameters with respect to ATP were found (Table 1), suggesting that changes in such parameters in response to phosphorylation or cyclin binding should be equivalent.

Kinetic parameters derived for histone H1 phosphorylation by the [T^{160}-P]CDK2−cyclin A (Figure 1) or [unP]CDK2−cyclin A (Figure 2) complex are listed in Table 2. To solve for the microscopic constants, k_2, k_{-2}, k_3, and k_4 (Scheme 1), initial velocity data were collected under varying concentrations of substrate as well as varied relative solvent

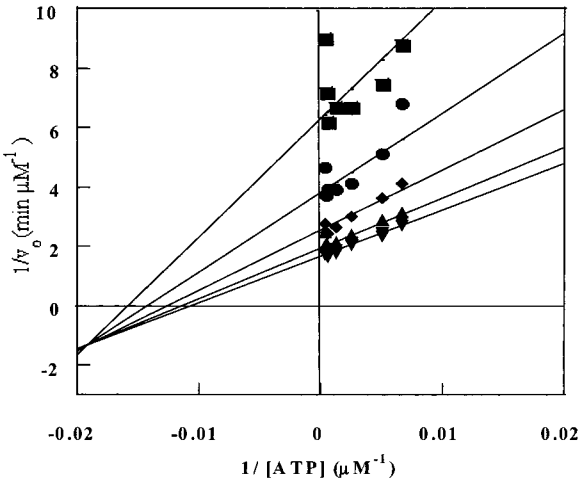

FIGURE 2: Dependence of the initial velocity of the [unP]CDK2−cyclin A complex on ATP and histone H1 concentration. Steady-state phosphorylation of histone H1 by the [unP]CDK2−cyclin A complex was assessed as a function of varied ATP concentration at 30 (■), 60 (●), 120 (◆), 240 (▲), and 420 μM histone H1 (▼). Equation 2 was globally fit to initial velocity data, and steady-state parameters were determined by nonlinear regression analysis. The best-fit curves are superimposed on the experimental data in double-reciprocal form. The optimized steady-state parameters are listed in Table 2.

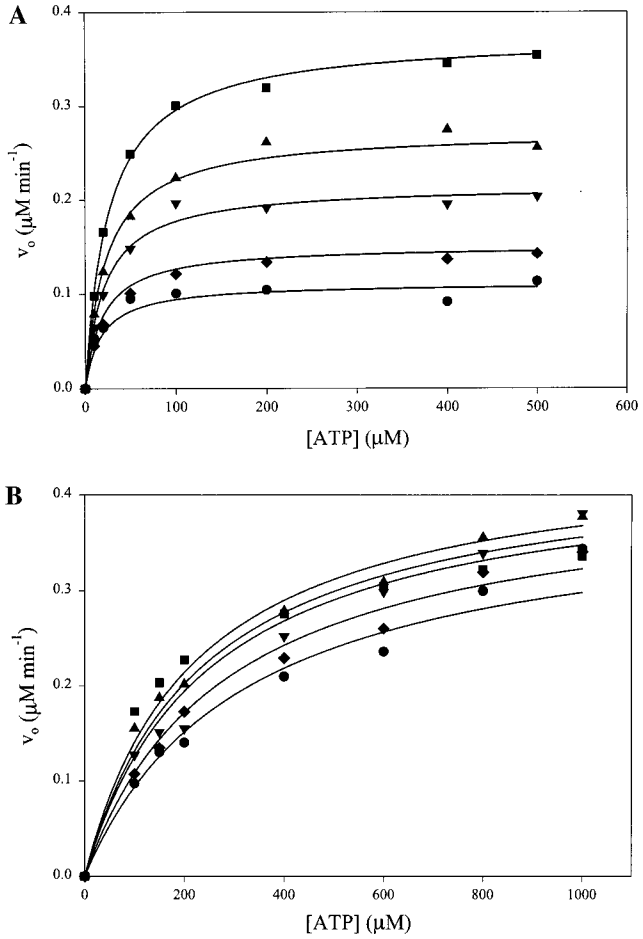

FIGURE 3: Dependence of steady-state kinetic parameters on relative solvent viscosity. The initial velocity for histone H1 phosphorylation was measured at saturating or near-saturating H1 concentrations, varied concentrations of ATP, and several fixed concentrations of sucrose (0−40%). Best-fit curves to the data obtained by nonlinear regression analysis are superimposed on the raw data points. The optimized rate constant values obtained by global fitting are listed in Table 2. (A) For the [T^{160}-P]CDK2−cyclin A complex, the histone H1 concentration was 20 μM; sucrose concentrations correspond to relative solvent viscosities (η_{rel}) of 1 (■), 1.5 (▲), 2 (▼), 3 (◆), and 4.2 (●). The concentration of the [T^{160}-P]CDK2−cyclin A complex was 2 nM. (B) For the [unP]CDK2−cyclin A complex, the histone H1 concentration was 400 μM. Relative solvent viscosities (η_{rel}) were 1 (■), 1.4 (▲), 1.8 (▼), 2.9 (◆), and 4.1 (●). The concentration of the [unP]CDK2−cyclin A complex was 1 μM.

viscosity, allowing all reaction steps to be isolated (see Materials and Methods) (Figure 3). We found that the K_d value (k_{-2}/k_2) for ATP was unchanged in response to phosphorylation [83 μM for the [unP]CDK2−cyclin A complex and 60 μM for the [T^{160}-P]CDK2−cyclin A complex (Table 2)]. On the other hand, phosphorylation results in a large rate enhancement of the phosphotransfer step (*10*; Table 2). This rate enhancement is seen only in the kinase reaction, and not in the ATPase reaction (*10*; Table 3). This suggests that phosphorylation of the CDK2−cyclin A complex at Thr^{160} serves principally to enhance the reactivity of the peptide or protein substrate, as opposed to that of ATP. While phosphorylation results in moderately enhanced affinity for a peptide substrate (*10*), neither the binding nor reactivity of ATP is affected.

Cyclin Binding to [unP]CDK2 Serves To Stabilize ATP. Evidence suggests that the physiological pathway for CDK2 activation consists of cyclin binding prior to phosphorylation (*14*, *15*). We therefore asked if cyclin binding in the first step of activation may serve to stabilize ATP. [unP]CDK2 displays no detectable kinase activity toward histone H1 (data not shown; also see refs *7* and *16*). Thus, the thermodynamic binding of ATP to [unP]CDK2·H1 could not be assessed by steady-state kinetic methods. To determine the possible effect of cyclin binding on aligning ATP for phosphoryl transfer, we isolated the phosphotransfer step in the ATPase reaction of CDK2 and the CDK2−cyclin A complex by solvent viscosometric analysis. Purified GST−CDK2 was immobilized on glutathione−agarose beads and subjected to incubation with either buffer or saturating quantities of cyclin A (Figure 4A). After elution, the specific ATPase activities were determined (Figure 4B). The [unP]CDK2−cyclin A complex displayed a turnover rate 25-fold higher than that of monomeric [unP]CDK2 (Figure 4B and Table 3). Because phosphorylation of the CDK2−cyclin A complex affects neither the rate of phosphoryl transfer in the ATPase reaction (k_3^{ATPase}) nor the binding of ATP (K_d^{ATP}) in the kinase reaction, we conclude that interaction of cyclin A with [unP]-CDK2 alone is sufficient for optimizing both these parameters.

Cyclin Binding to [T^{160}-P]CDK2 Enhances Substrate Binding but Not Turnover. To comprehensively define the structure−function relationship between phosphorylation, cyclin binding, and catalytic activation, we characterized the kinetic reaction pathway of the CDK2 monomer phosphorylated at Thr^{160} ([T^{160}-P]CDK2). The k_{cat} value for [T^{160}-P]CDK2 (Figure 5) was found to be only 8-fold lower than that for the [T^{160}-P]CDK2−cyclin A complex (Tables 2 and 4), demonstrating that cyclin had little effect on turnover. By comparison, the binding affinity for histone H1 was enhanced more than 480-fold (Tables 2 and 4). Thus, with respect to the phosphorylation of histone H1, [T^{160}-P]-CDK2 (but not [unP]CDK2) is defective mainly in ground-state binding. Catalytic turnover is largely unimpaired.

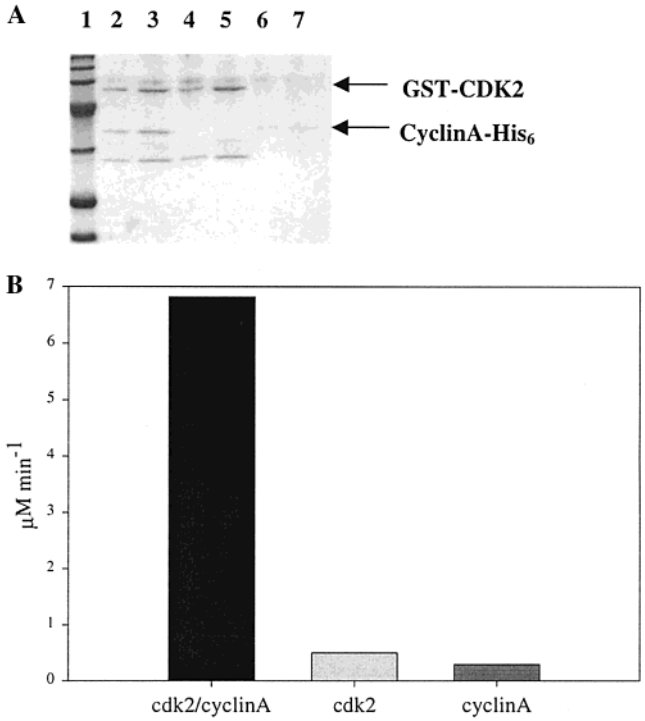

FIGURE 4: Effect of cyclin binding on ATPase activity. Glutathione−agarose beads were loaded with GST-bound [unP]CDK2, washed, and then loaded with cyclin A or buffer, as described in Materials and Methods. Proteins were eluted with glutathione and analyzed by SDS−PAGE (12.5% acrylamide). (A) Lane 1, molecular mass standards (200, 97.4, 68, 43, 29, 18.4, and 14.3 kDa, from top to bottom). Lanes 2 and 3, 2 and 4 μL, respectively, of eluate from beads loaded with GST-bound [unP]CDK2 and cyclin A. Lanes 4 and 5, 2 and 4 μL, respectively, of eluate from beads loaded with GST-bound [unP]CDK2 alone. Lanes 6 and 7, 2 and 4 μL, respectively, of eluate from beads loaded with cyclin A alone. (B) Samples described for panel A were assayed for ATPase activity as described in Materials and Methods.

DISCUSSION

We have sought to elucidate the complete catalytic reaction pathway for the activation of CDK2 by interaction with cyclin A and phosphorylation at Thr^{160}. To achieve this, we attempted to measure all kinetic parameters (Scheme 1) for all forms of CDK2 (Figure 6A). A limitation of these studies was the complete lack of detectable kinase activity found for the [unP]CDK2 species. Thus, not all parameters for the complete pathway to activation could be obtained. However, the available data together with crystallographic information depict a general scheme describing the kinetic role of cyclin binding versus Thr^{160} phosphorylation in the activation process.

Equilibrium binding (*6*) as well as X-ray crystallographic data (*3*, *4*, *6*) show that either histone H1 or ATP can add to the CDK2 active site first. Thus, the kinetic mechanism of CDK2 is predicted to be random. Scheme 1 depicts the addition of substrate followed by catalytic turnover when the alternate substrate is held at saturation. To determine the kinetic effects of cyclin binding or phosphorylation on the individual reaction steps, we employed steady-state solvent viscosometric techniques.

Our data reveal that the respective roles of cyclin binding versus phosphorylation in the activation of CDK2 are not cleanly separable in terms of their kinetic effects. For example, while the binding of ATP and its reactivity are controlled exclusively by interaction with cyclin along pathway 1−2 (Figure 6A), both phosphorylation and cyclin binding are required for complete stabilization of ATP along pathway 3−4 (Figure 6A and Table 4). Similarly, while phosphorylation affects only histone H1 (or peptide) binding

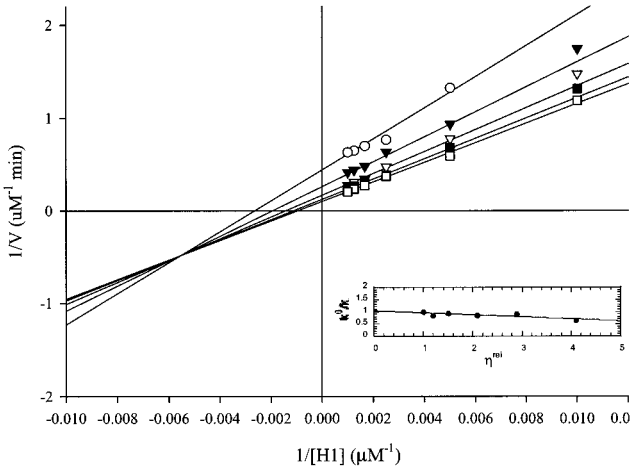

FIGURE 5: Dependence of the initial velocity of [T^{160}-P]CDK2 on ATP and histone H1 concentration. Steady-state phosphorylation of histone H1 by [T^{160}-P]CDK2 (0.5 μM) was assessed as a function of varied histone H1 concentration at 0.2 (○), 0.4 (▼), 0.8 (▽), 1.6 (■), and 3.2 mM ATP (□). Equation 2 was globally fit to initial velocity data, and steady-state parameters were determined by nonlinear regression analysis. The best-fit curves are superimposed on the experimental data in double-reciprocal form. The optimized steady-state parameters are listed in Table 1. The inset shows histone phosphorylation as determined using 1 μM [T^{160}-P]CDK2, 400 μM histone H1, 4.5 mM ATP, and varied sucrose concentrations. k^0/k is the fold decrease in k_{cat}/K_m^{H1} as a function of relative solvent viscosity (η_{rel}).

Table 1: Kinetic Parameters for the [T^{160}-P]CDK2−Cyclin A Complex (Peptide vs Histone H1 Phosphorylation)

parameter	peptide (PKTPKKAKKL)	histone H1
k_{cat} (s^{-1})	7 ± 4	3.5 ± 0.5
K_m (μM)	8 ± 0.7	≤ 0.8
K_m^{ATP} (μM)	55 ± 5	25 ± 5
k_{cat}/K_m^{η}(ATP)	0.6 ± 0.2	0.4 ± 0.12
$k_{2(ATP)}$ ($\mu M^{-1}\,s^{-1}$)	0.2 ± 0.1	0.3 ± 0.1
$k_{-2(ATP)}$ (s^{-1})	30 ± 5	20 ± 5
k_{cat}^{η}	0.8 ± 0.3	0.7 ± 0.12
k_3 (s^{-1})	35 ± 16	13 ± 4
k_4 (s^{-1})	9 ± 3	4 ± 1

Table 2: Kinetic Parameters for Histone H1 Phosphorylation

parameter	[unP]CDK2−cyclin A	[T^{160}-P]CDK2	[T^{160}-P]CDK2−cyclin A
k_{cat} (s^{-1})	0.013 ± 0.006	0.4 ± 0.1	3.5 ± 0.5
K_m^{H1} (μM)	115 ± 30	1000−2000	≤ 0.8
K_m^{ATP} (μM)	106 ± 24	920 ± 300	25 ± 5
k_{cat}/K_m^{η}(ATP)	0.2 ± 0.08	nd[c]	0.4 ± 0.12
k_{cat}/K_m^{η}(H1)	0.17 ± 0.05	-0.1 ± 0.05	nd[c]
k_{cat}^{η}	0.01 ± 0.03	nd[c]	0.7 ± 0.12
K_d^{ATP} (μM)	83 ± 30[a]	nd[c]	60[a] ± 20
K_d^{H1} (μM)	95 ± 30[a]	≥ 1300[a]	≤ 2.7[a]
k_2^{ATP} ($\mu M^{-1}\,s^{-1}$)	0.0006 ± 0.0002	nd[c]	0.3 ± 0.1
k_{-2}^{ATP} (s^{-1})	0.05 ± 0.01	nd[c]	20 ± 5
k_3 (s^{-1})	0.013 ± 0.005	≥ 0.4[b]	13 ± 2
k_4 (s^{-1})	nd[c]	nd[c]	4 ± 1

[a] $K_d = K_m(1 - k_{cat}/K_m^{\eta})/(1 - k_{cat}^{\eta})$. [b] $k_3 = k_{cat}/(1 - k_{cat}^{\eta})$. [c] Could not be determined.

Table 3: Kinetic Parameters for the ATPase Reaction

	[unP]CDK2	[unP]CDK2−cyclin A	[T^{160}P]CDK2	[T^{160}P]CDK2−cyclin A
K_m^{ATP} (μM)		80 ± 5	190 ± 40	
k_{cat} (min^{-1})	0.4 ± 0.2	10 ± 4[a]	13 ± 2	12 ± 3[a]
k_{cat}^{η}	−0.1 ± 0.05		0.05 ± 0.03	
k_3 (min^{-1})	0.4 ± 0.2	10 ± 4[a]	13 ± 2	12 ± 3[a]

[a] Taken from ref *10*.

Table 4: Fold Change in Kinetic Parameters for Activation of CDK2

	activation step[a] 1	activation step[a] 2	activation step[a] 3	activation step[a] 4
k_{cat} (s^{-1})		270		8.8
k_3 (s^{-1})		1000		≤32
K_m^{H1} (μM)		≥144		≥1625
K_d^{H1} (μM)		≥35		≥480
K_m^{ATP} (μM)		4.2		37
K_d^{ATP} (μM)		1.4		nd[b]
k_{cat}^{ATPase} (min^{-1})	25	1.2	32	1.1
k_3^{ATPase} (min^{-1})	25	1.2	32	1.1

[a] See Figure 6A. [b] Could not be determined.

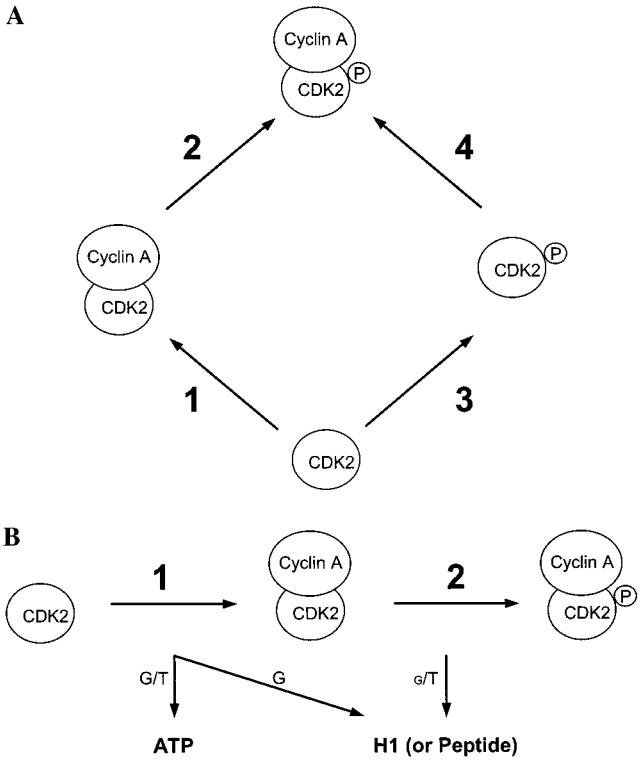

FIGURE 6: (A) Pathways for activation of CDK2 in response to cyclin binding and phosphorylation at Thr^{160}. The physiologic pathway consists of step 1 followed by step 2. (B) In step 1, interaction with cyclin serves to enhance ATP binding in both the ground and transition states. In addition, large effects on ground-state binding of the protein−peptide substrate with minimal effects on turnover are predicted. In step 2, phosphorylation serves principally to stabilize the protein−peptide substrate in the transition state with moderate effects on ground-state binding. G, ground-state binding effects; T, transition-state binding effects.

and the reactivity of this substrate along pathway 1−2, it serves to align ATP for phosphotransfer along pathway 3−4 (Table 4). Clearly, net activation is the result of significant synergy between cyclin binding and phosphorylation.

While either pathway is theoretically possible, evidence strongly suggests that in mammalian cells cyclin binding precedes phosphorylation (*14*, *15*). Among the evidence, mammalian CAK, as opposed to that from yeast, phosphorylates monomeric CDK2 extremely poorly in comparison to the CDK2−cyclin A complex (*15*), and monomeric [T^{160}-P]CDK2 from mammalian cells has not been reported (M. Solomon, personal communication). When pathway 1−2 is considered (Figure 6A), phosphorylation of the CDK2−cyclin A complex serves only to moderately enhance the binding (K_d), but greatly enhance the reactivity (k_3) of protein or peptide substrates. Phosphorylation has no effect on either ATP binding affinity (K_d^{ATP}) or its reactivity for phosphoryl transfer (k_3^{ATPase}) (Table 4) (see also ref *17*). Thus, it is assumed that these parameters are optimized by cyclin binding. We show that cyclin plays two roles in the putative in vivo pathway to CDK2 activation.

(1) Maximal Stabilization of ATP. While K_d^{ATP} for [unP]-CDK2 could not be determined in steady-state kinetic assays, enhanced affinity between [unP]CDK2 and a fluorescent nucleotide derivative, mantATP, in response to cyclin A binding, has previously been demonstrated by fluorescence equilibrium binding methods (*18*). Our data extend this observation by demonstrating that ATP binding is also significantly stabilized in the transition state for phosphoryl transfer (Figure 4). Therefore, since phosphorylation (Figure 6A, step 2) has no effect on ATP binding energy (in the ground or transition state), we conclude that all kinetic parameters linked to ATP are optimized in response to interaction with cyclin (Figure 6A, step 1).

(2) Stabilization of the Protein Substrate. While interaction of cyclin with CDK2 provides complete stabilization of ATP, our data indicate that enormous stabilization of histone H1 also occurs. This is consistent with the CDK2 structure, in which cyclin binding dramatically reorients the activation loop (*3*) that otherwise blocks access of a peptide substrate to the active site (*7*). While the K_d value for H1 could not be measured on [unP]CDK2, precluding determination of the fold effect of cyclin binding on this parameter (Figure 6A, step 1), cyclin binding increased the affinity of histone H1 for [T^{160}-P]CDK2 (Figure 6A, step 4) by more than 480-fold (Table 4). The 480-fold enhancement is a lower limit derived directly from the K_m value of the [T^{160}-P]CDK2−cyclin A complex for histone H1, estimated to be ≤0.8 μM. The likelihood that the true K_m value may be less than 0.8 μM would directly translate to a proportionally lower K_d^{H1} value. Thus, the precise extent to which histone H1 binding is stabilized in response to cyclin may be significantly greater than the lower limit of 480-fold. Although we have been able to access the kinetic effects of cyclin binding on [T^{160}-P]CDK2 only, we propose that the effects on stabilizing histone H1 binding with respect to [unP]CDK2 will be similar.

The activity of [T^{160}-P]CDK2 was previously reported to be 0.3% of that of the fully active enzyme measured under subsaturating concentrations of both histone H1 and ATP (*6*). At saturating levels of both substrates, we have found that the true k_{cat} value of [T^{160}-P]CDK2 is only 8-fold lower that that of the [T^{160}-P]CDK2−cyclin A complex. Thus, in comparison to the large effect on histone binding affinity, there is only a minor effect on the overall turnover rate (k_{cat}) in response to cyclin binding (Table 4). Therefore, the low

activity of [T^{160}-P]CDK2 may be interpreted as being the result of a simple competitive inhibition mechanism.

A competitive pattern of inhibition is observed when a large fraction of the total enzyme existing in an inactive form can be completely driven to the active state by saturating substrate levels. In the case of [T^{160}-P]CDK2, the activation loop is highly disordered (*6*), suggesting that in the absence of cyclin the active conformer is necessarily a poorly populated species. We propose that histone H1 alone, if present at a sufficiently high concentration, is sufficient to nearly fully populate the active conformation. In vivo, this function is performed by cyclin binding, which, as a consequence, dramatically lowers the K_m value for histone. While [T^{160}-P]CDK2 shows minimal defect in catalytic turnover, the conformation of the activation loop in unphosphorylated CDK2 is such that *both* substrate binding and catalytic turnover are severely debilitated, hence the complete inactivity of the [unP]CDK2 monomer.

In summary, the putative physiological pathway to CDK2 activation consists of the initial binding of cyclin A to the CDK2 catalytic subunit (*14*, *15*), resulting in a complex with partial enzyme activity (*16*) (Figure 6B). The partial increase in the catalytic rate is due to maximal enhancement of ATP binding, as well as the optimized alignment of ATP in the transition state for phosphotransfer. The latter may be attributed to repositioning of the PSTAIRE helix promoting alignment of Glu^{51} with Lys^{33}, which crucially aligns the α- and β-phosphoryl group oxygens of ATP for chemical transfer (*3*). Second, cyclin binding also causes greatly enhanced affinity for the protein or peptide substrate by providing the energy required to correctly configure the activation loop. This is inferred from crystallographic data (*3*), as well as from the observed large increase in binding affinity of histone H1 for [T^{160}-P]CDK2 (Figure 6A, step 4).

Full activation of the CDK2−cyclin A dimer requires phosphorylation of CDK2 at Thr^{160}. Phosphorylation results in rotation of the carbonyl group of Val^{163} out of the active site P_{+1} binding pocket (*7*), which correlates with a moderate (50-fold) enhancement in peptide substrate binding affinity, revealed by kinetic analysis (*10*). However, the large increase in overall catalytic power arises mostly from a 1000−3000-fold increase in the phosphoryl group transfer rate [Table 4 (*10*)]. Thus, the main effect of phosphorylation is not to enhance ground-state binding, but rather to stabilize the peptide or protein substrate in the transition state for phosphoryl transfer.

In conclusion, our studies provide an essential framework in which the atomic structure and biochemical regulation of the cyclin-dependent kinases, and protein kinases in general, may be correlated in detail. Important studies for the future, in terms of the structure−activity relationship of this family of enzymes, will include the identification of key active site residues and relevant conformational changes or correlated motions along the kinetic reaction pathway, and the role of these parameters in catalytic regulation.

ACKNOWLEDGMENT

We are deeply grateful to Nick Brown and Louise Johnson (Laboratory of Molecular Biophysics, University of Oxford, Oxford, England) for providing [T^{160}-P]CDK2 protein. We thank Matt Kirtley who carried out preliminary studies.

REFERENCES

1. Morgan, D. O. (1997) *Annu. Rev. Cell Dev. Biol. 13*, 261−291.
2. Morgan, D. O. (1995) *Nature 374*, 131−134.
3. Jeffrey, P. D., Russo, A. A., Polyak, K., Gibbs, E., Hurwitz, J., Massague, J., and Pavletich, N. P. (1995) *Nature 376*, 313−320.
4. Russo, A. A., Jeffrey, P. D., and Pavletich, N. P. (1996) *Nat. Struct. Biol. 3*, 696−700.
5. De Bondt, H. L., Rosenblatt, J., Jancarik, J., Jones, H. D., Morgan, D. O., and Kim, S. H. (1993) *Nature 363*, 595−602.
6. Brown, N. R., Noble, M. E., Lawrie, A. M., Morris, M. C., Tunnah, P., Divita, G., Johnson, L. N., and Endicott, J. A. (1999) *J. Biol. Chem. 274*, 8746−8756.
7. Brown, N. R., Noble, M. E. M., Endicott, J. A., and Johnson, L. N. (1999) *Nat. Cell Biol. 1*, 438−443.
8. Pavletich, N. P. (1999) *J. Mol. Biol. 287*, 821−828.
9. Smith, C. M., Radzio-Andzelm, E., Madhusudan, Akamine, P., and Taylor, S. S. (1999) *Prog. Biophys. Mol. Biol. 71*, 313−341.
10. Hagopian, J. C., Kirtley, M. P., Stevenson, L. M., Gergis, R. M., Russo, A. A., Pavletich, N. P., Parsons, S. M., and Lew, J. (2001) *J. Biol. Chem. 276*, 275−280.
11. Prowse, C. N., Hagopian, J. C., Cobb, M. H., Ahn, N. G., and Lew, J. (2000) *Biochemistry 39*, 6258−6266.
12. Nakatani, H., and Dunford, H. B. (1979) *J. Phys. Chem. 83*, 2662−2665.
13. Prowse, C. N., and Lew, J. (2001) *J. Biol. Chem. 276*, 99−103.
14. Cheng, A., Ross, K. E., Kaldis, P., and Solomon, M. J. (1999) *Genes Dev. 13*, 2946−2957.
15. Kaldis, P., Russo, A. A., Chou, H. S., Pavletich, N. P., and Solomon, M. J. (1998) *Mol. Biol. Cell 9*, 2545−2560.
16. Connell-Crowley, L., Solomon, M. J., Wei, N., and Harper, J. W. (1993) *Mol. Biol. Cell 4*, 79−92.
17. Holmes, J. K., and Solomon, M. J. (2001) *Eur. J. Biochem. 268*, 4647−4652.
18. Heitz, F., Morris, M. C., Fesquet, D., Cavadore, J. C., Doree, M., and Divita, G. (1997) *Biochemistry 36*, 4995−5003.

BI025812H